ADVANCED FUNCTIONAL MATERIALS
www.afm-journal.de

www.MaterialsViews.com

Responsive Macroscopic Materials From Self-Assembled Cross-Linked SiO_2-PNIPAAm Core/Shell Structures

Christian W. Pester, Artjom Konradi, Birte Varnholt, Patrick van Rijn, and Alexander Böker*

A way to obtain macroscopic responsive materials from silicon-oxide polymer core/shell microstructures is presented. The microparticles are composed of a 60 nm SiO_2-core with a random copolymer corona of the temperature responsive poly-*N*-isopropylacrylamide (PNIPAAm) and the UV-cross-linkable 2-(dimethyl maleinimido)-*N*-ethyl-acrylamide. The particles shrink upon heating and form a stable gel in both water and tetrahydrofuran (THF) at 3–5 wt% particle content. Cross-linking the aqueous gel results in shrinkage when the temperature is increased above the lower critical solution temperature and it regains its original size upon cooling. By freeze drying with subsequent UV irradiation, thin stable layers are prepared. Stable fibers are produced by extruding a THF gel into water and subsequent UV irradiation, harnessing the cononsolvency effect of PNIPAAm in water/THF mixtures. The temperature responsiveness translates to the macroscopic materials as both films and fibers show the same collapsing behavior as the microcore/shell particle. The collapse and re-swelling of the materials is related to the expelling and re-uptake of water, which is used to incorporate gold nanoparticles into the materials by a simple heating/cooling cycle. This allows for future applications, as various functional particles (antibacterial, fluorescence, catalysis, etc.) can easily be incorporated in these systems.

1. Introduction

Smart systems are essential for the development of new functional materials due their responsiveness to external stimuli.[1–3] This responsiveness allows materials to be switched between different states; most often between solubilized and non-solubilized, which, in general, induces aggregation. However, the effects are mostly confined to spherical nano- and microstructures[4,5] and surface confined thin films[4–7] and it remains challenging to process the nano- or microstructures into macroscopic materials.[8,9] Nonetheless, significant advances have been made recently with wrinkle-guided microgel-fiber formation with fiber lengths several orders of magnitude larger than their thickness.[10]

C. W. Pester, A. Konradi, B. Varnholt, Dr. P. van Rijn, Prof. A. Böker
DWI an der RWTH Aachen e.V., Lehrstuhl
für Makromolekulare Materialien und Oberflächen
RWTH Aachen University
Forckenbeckstrasse 50, 52056 Aachen, Germany
E-mail: vanrijn@dwi.rwth-aachen.de

DOI: 10.1002/adfm.201102802

Switching between states can be induced by a change in pH,[11] temperature,[12] ionic strength,[13] or light.[14] It can be performed in systems composed of small molecular components[15] as well as in polymeric systems.[16,17] Especially the latter are very attractive as they pose the possibility of a cooperative effect: an effect induced by multiple monomeric subunits inside a polymeric strand induces a larger, and often a more controlled and directed effect than the single monomers alone. Well-known polymeric systems with this type of cooperative effect are based on poly-*N*-isopropylacrylamide (PNIPAAm). Responsive systems composed of PNIPAAm are able to alter their morphology when the temperature is changed, due to the polymer's lower critical solution temperature (LCST) in water, rendering it insoluble at elevated temperatures.[18,19]

Cross-linked PNIPAAm in water is able to form macroscopic gels, leading to a system that can be to switch between different gelated, soluble and insoluble states.[20,21] When heated, the system collapses and upon cooling the system re-absorbs the water and swells again (LCST behavior). This feature has been particularly attractive in aqueous microgel systems,[22] a well-defined nano- to microscaled spherical system composed of polymers with about 90% of the total mass consisting of entrapped solvent.[23] These confined responsive gel systems are attractive for delivery purposes[24] and are also often used in core/shell structures.[25] The collapsing of the polymers around a central core induces a controlled motion of the polymers, resulting in a decrease in diameter. In such structures, the core is of a different nano-sized material[26] e.g., polymeric,[27] inorganic (SiO_2,[28] Au,[29,30] Ag,[31] semiconductor materials,[32] Fe[33,34]), or even proteins.[35,36] The inner core adds new functionalities to the microgel-like structure in the form of either light-triggered heat dissipation (Au, specific plasmon absorption),[37] antibacterial properties (Ag, release of Ag-ions),[38,39] or fluorescence (CdS/Se, quantum dots).[40] Consequently, polymer–nanoparticle hybrid materials are an interesting class of materials, uniquely enhancing the properties and responsiveness of polymeric materials, even when not covalently bound.[41–44]

Here we discuss the fabrication of macroscopic materials in the form of fibers and thin membrane-like films using

SiO_2-PNIPAAm core/shell microparticles with 2-(dimethyl maleinimido)-*N*-ethyl-acrylamide (DMIAAm) as an additional photoresponsive cross-linker.[45] The temperature responsiveness of SiO_2-PNIPAAm particles is translated to the macroscopic materials, enabling the reversible collapse and swelling of these materials induced by a change in temperature. The collapse and re-swelling was found to be a very convenient way of incorporating other nanomaterials, which remained confined inside the SiO_2-PNIPAAm macroscopic material after re-swelling. This approach is more versatile than the synthesis of nanostructures inside polymer matrices.[46] The materials were formed utilizing freeze-drying and the cononsolvency effect, the insolubility of PNIPAAm in different solvent compositions.

These systems will have a significant impact on preparing various new materials which can be used for reactive membranes, reactive fibers, and, due to the affinity of cells towards PNIPAAm, it would also allow for the use as cell-culture scaffolds.[47]

2. Results and Discussion

2.1. Synthesis and Characterization of SiO_2-Polymer Core/Shell Microstructures

Compared to other reported core/shell structures,[28,48] there are three distinct differences comprised in the present system: first of all there is the lack of a conventional cross-linker, which binds the polymer chains to each other covalently around the inner core. In general, a *bis*-acrylamide is used and it provides the features necessary to produce a microgel particle. The cross-linking creates a network which accommodates significant amounts of solvent but also inhibits the polymer chains from moving freely. Second, the polymerization was performed with a higher monomer-to-surface initiator ratio, in this case NIPAAm, which provides a shell around the inner SiO_2-core that is much thicker than usually grown. Third, in addition to NIPAAm, a photoresponsive cross-linker has been copolymerized to obtain a random copolymer. The cross-linker is able to induce interchain cross-linking with polymer chains attached to the same SiO_2-nanoparticle as well as between different particles. Especially the latter enables the production of macroscopic stable structures.

PNIPAAm, being an LCST system, can be switched between hydrophilic and hydrophobic via changes in temperature.[20,21] Such responsiveness on the microstructure level (**Scheme 1**) is also reflected in the macroscopic material. The DMIAAm is able to engage in a [2 + 2]-photocyclization reaction with another DMIAAm moiety, thereby creating a covalently bound system (Scheme 1), even after additional processing such as drying and extrusion.

The SiO_2-$(PNIPAAm)_{100}(DMIAAm)_5$ (subscripts depict relative molar ratio) were synthesized from SiO_2-nanoparticles followed by surface modification with methacryloxypropyltrimethoxysilane (MPS) and subsequent emulsion copolymerization with NIPAAm and DMIAAm (Scheme 1).[28] The SiO_2 core nanoparticles were synthesized by the well-known

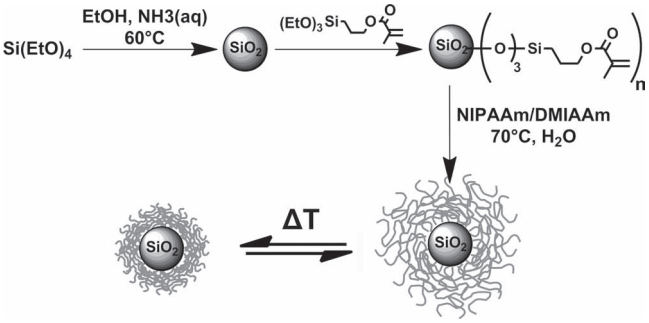

Scheme 1. Synthetic route for the temperature-responsive SiO_2-polymer core/shell structures. The SiO_2 nanoparticle core is synthesized via the Stöber procedure[49] followed by surface modification and polymerization. Upon raising the temperature above the LCST, the PNIPAAm shell collapses around the core due to dehydration of the polymer.

Stöber method from tetraethoxysilane in ethanol (EtOH) and ammonia, as shown in Scheme 1.[49] The particle diameter was found to be approximately 60 ± 3 nm (**Figure 1**A).

In our case, a tenfold excess of monomer was used and the *bis*-acrylamide cross-linker was omitted. This results in core/shell particles with an extremely thick polymer shell. This finding is rather surprising for a free radical polymerization. One explanation could be the formation of an emulsion during the polymerization (above the LCST of the polymer), which produces a confined space with higher viscosity influencing the reaction with respect to termination and conversion. This is known as the Trommsdorff–Norish effect or gel effect and causes autoacceleration of the reaction.[66] Also this may lead to interchain side reactions resulting in cross-linking that would add to the stability of the shell even without the addition of a cross-linker. Still, a higher individual polymer chain flexibility is obtained in comparison to the systems where the grafted chains form a covalently bound network due to the addition of a cross-linker (e.g., *bis*-acrylamide). This synthetic protocol provides core/shell particles with a diameter of approximately 1 µm as determined from dried particles by transmission electron microscopy (TEM) (Figure 1B,C). The particles display a difference in density, which could be a drying effect during sample preparation, but are quite homogeneous in size. While some particles contain more than one core per core/shell structure, in most cases there is only one core present (Figure 1B,C).

Dynamic light scattering (DLS) showed significantly larger particle sizes (≈3–3.3 µm, **Figure 2**) in solution (≈0.1 mg mL^{-1} in

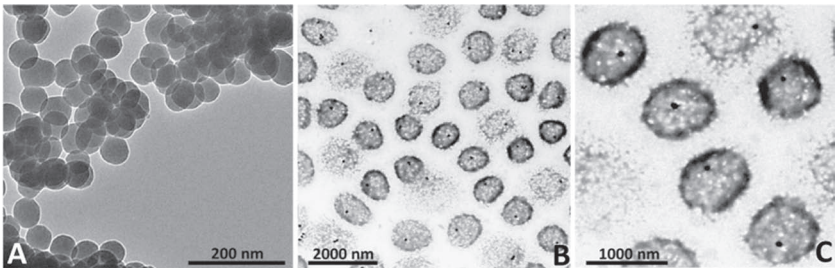

Figure 1. TEM images of the synthesized SiO_2-nanoparticles of 60 nm in diameter (A) and the core/shell microstructures of about 1 µm after polymerization (B,C).

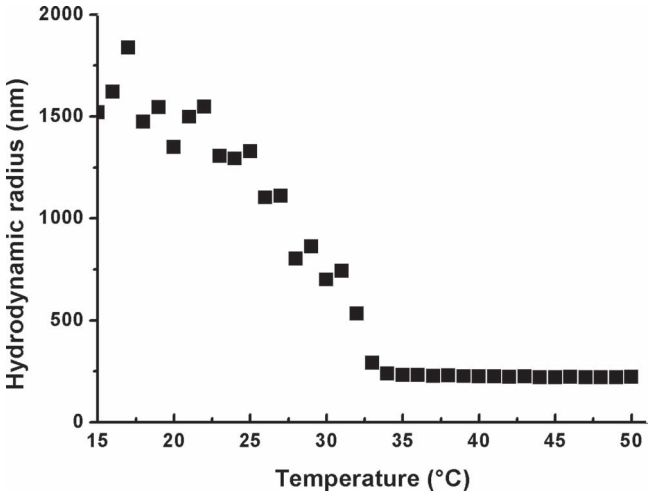

Figure 2. Hydrodynamic radius analyzed by DLS at various temperatures. The radius decreases gradually with increasing temperature from about 1.5–1.8 µm to ≈220 nm due to the collapse of the PNIPAAm shell.

MilliQ-water) at temperatures between 15 and 20 °C. The hydrodynamic radius is inversely proportional to the temperature and steadily decreases until it reaches a plateau value of about 220 nm at 34 °C where the shell is fully collapsed. In solution the particles decrease down to 12% of their original size, which is similar to previously reported inorganic core/polymer shell structures.[28,48,50] As particle densities vary (cf. TEM images), their diameter determined by DLS fluctuates at low temperatures.

2.2. Gelation Properties

It was found that at high SiO_2-PNIPAAm-DMIAAm particle concentration the solution displayed such a high viscosity that flow was inhibited. A gel-like substance was obtained that can endure the inverted test tube test for several weeks without showing any sign of flow (**Figure 3**A). It is possible that, instead of fiber-like networks as is seen for low-molecular-weight component

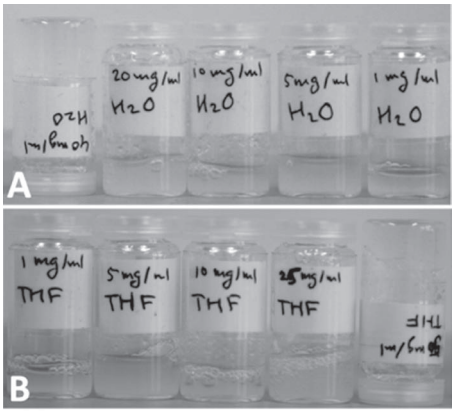

Figure 3. Photographs of SiO_2-PNIPAAm-DMIAAm particles at concentration of (from left to right) 40, 20, 10, 5, and 1 mg mL^{-1} in water (A) and of 1, 5, 10, 25, and 50 mg mL^{-1} in THF (B). At the highest concentrations stable gels were formed that did not have any noticeable flow.

systems,[15] the nature of the soft-particle colloids transforms the colloidal solution to an "attractive" glass state (particle gel) that induces solidification and provides tunable mechanical properties to the system.[51] The concentration of the core/shell particles was determined by freeze-drying 10 mL of gel and weighing the dry content. It was found that the dry weight was about 40 mg mL^{-1} of gel (≈4 wt%). From the gel of 40 mg mL^{-1}, a dilution series was prepared to investigate the critical gelation concentration (cgc). The dilution was performed by adding the appropriate volume of MilliQ-water to the gel after which the sample was repeatedly sonicated and vortexed until a homogeneous gel/solution was obtained. From this series it was found that the cgc is at approximately 31 mg mL^{-1}, as below this concentration the gel starts to display a flow.

Attempts were also made to prepare a highly concentrated solution in tetrahydrofuran (THF), using freeze-dried core/shell particles and mix this in water to obtain a defined concentration since it proved difficult to solubilize the freeze-dried particles. However, an unexpected gelation process occurred. At a comparable concentration (≈50 mg mL^{-1}) with respect to water, SiO_2-PNIPAAm-DMIAAm also gelates THF, inhibiting the flow of the solution (Figure 3B). Other solvents, both polar and non-polar, were examined and it was found that ethanol, toluene, and dimethylformamide (DMF) were also able to be gelated at 50 mg mL^{-1} while dichloromethane (DCM) did not gelate but gave a white suspension instead (**Table 1**, Supporting Information SI 1).

The polymer shell around the SiO_2-core contains two responsive components: DMIAAm, which is UV-responsive and is able to covalently cross-link when irradiated with UV-light, and PNIPAAm, which has thermosensitive properties. According to this, the hydrogel composed of the core/shell particles was irradiated with UV light while cooling at 0 °C to prevent the gel from being heated above its LCST. The irradiation was performed for three hours due to the high turbidity of the sample. Whilst, there was no visible difference between the cross-linked and the non-cross-linked gels, analysis by cryogenic scanning

Table 1. Gelation behavior of SiO_2-PNIPAAm-DMIAAm (cross-linked (c.-l.)) in different solvents, concentrations, and temperatures. Gel (G), turbid gel (TG), weak gel (WG), sticky gel (SG), reduced gel due to solvent evaporation (RG), viscous solution (VS), turbid solution (TS), gel collapses and swells again after cooling (shrink).

Solvent	Concentration [mg mL^{-1}]	4 °C	20 °C	50 °C	20 °C (after heating)	20 °C c.-l.	50 °C c.-l.
H_2O	40	G	TG	MS	TG	TG	shrink
	<31	WG	VS	MS	VS	—	—
	<10	VS	TS	MS	TS	—	—
THF	50	TG	TG	TG	TG	TG	TG
	25	TS	TS	TS	TS	—	—
	10	TS	TS	TS	TS	—	—
DMF	50	G	G	G	TG	G	G
Toluene	50	G	SG	G	SG	G	G
EtOH	50	G	WG	RG	—	G	RG
DCM	50	SG	TS	RG	—	—	—

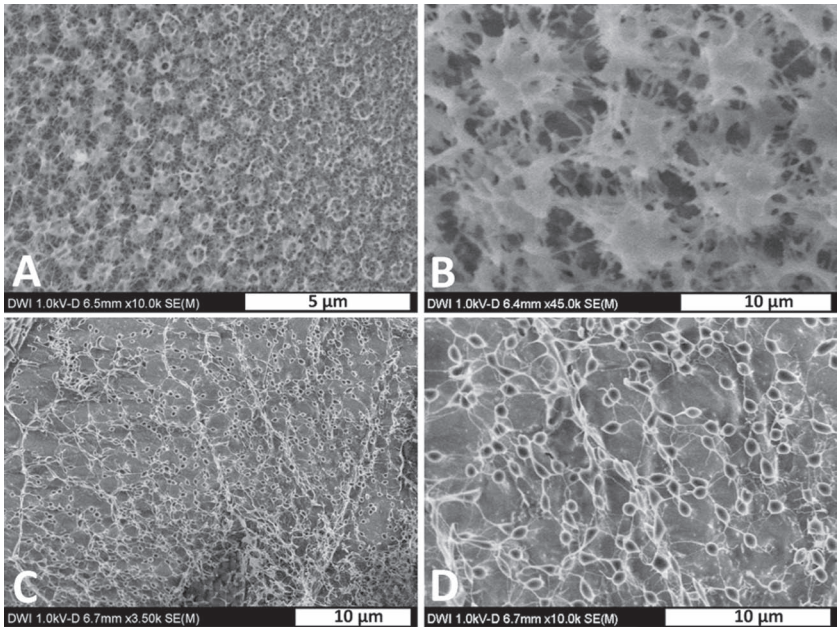

Figure 4. Cryo-SEM images of non-cross-linked (A,B) and cross-linked gels (C,D) in water at 40 mg mL^{-1}. Although the visual appearances of the gels are very similar, the microstructure deviates significantly. The non-cross-linked gel has a regular distribution of micrometer-sized low density structures; the cross-linked gel has smaller, denser spheres that appear to be connected via thin polymer fibers.

electron microscopy (cryo-SEM) allowed for observation of a clear difference in morphology (**Figure 4**). The non-cross-linked hydrogel displayed a closely packed ordering of spherical low-density structures, the cross-linked gel showed smaller and denser spherical structures connected by thin fibers. This is expected for intraparticle cross-linking in combination with interparticle cross-linking. Even though the morphology changes significantly on a microscopic level, the gel appears opaque and behaves similar (inhibited flow) at room temperature (Supporting Information SI 2).

PNIPAAm will undergo a transition from its hydrated to its insoluble form upon raising the temperature above its LCST (≈30–35 °C). Both cross-linked and non-cross-linked gels in water as well as in THF were investigated for their visual appearances and behavior at both ambient temperature and 50 °C, studying the materials' thermoresponsiveness. At ambient temperature, gels were observed at 50 and 40 mg mL^{-1} in both THF and water. Both gels were whitish in color and the aqueous gel was slightly less transparent (**Figure 5**A). In contrast to the THF gel, increasing the temperature of the aqueous gel to 50 °C transforms the sample into a milky suspension while the THF gel remained transparent and non-flowing. After cross-linking via UV irradiation, neither gel showed any difference in appearance or behavior at ambient temperature and while the THF gel was not influenced by increasing temperature, the cross-linked aqueous gel turned white and shrank (Figure 5C). This produced a lump of gel with a rubbery appearance that could be taken from the vial (Supporting Information SI 5). The lump of gel slowly became more transparent upon cooling from 50 °C to room temperature but remained stable (Supporting Information SI 5). A shrunken gel left undisturbed while cooling adopts its previous shape again and displays the same nonflowing properties and transparency as before.

In the following, we will describe two processing approaches that were followed to fabricate macroscopic structures in order to conveniently project the thermoresponsive properties of the microparticles onto the macroscopic materials.

2.3. Responsive Thin Films

The first approach was creating a thin film by taking the viscous solution of the particles in water and distributing it over a large surface while freezing it with liquid nitrogen. The frozen thin film was then freeze-dried in order to remove all water, leaving behind a rather fluffy and flexible thin film that could easily be handled without tearing or breaking (Supporting Information SI 3). The obtained material was treated with UV irradiation for 4–5 hours in order to cross-link the particles. This treatment adds stability and allows for rehydration without destruction of the superstructure. Both cross-linked and non-cross-linked materials were added to water and at first both were hydrated and remained intact. However, while the non-cross-linked layer loses its integrity and slowly dissipates, spreading across the water surface (**Figure 6**A), the cross-linked material remained stable for several weeks, even when mildly shaken (Figure 6B).

The film could even be lifted with tweezers, immediately reshaping when re-submersed in water. The cross-linked film was lifted onto a flat silicon-substrate and analyzed in the dried state by scanning force microscopy (SFM) (**Figure 7**A–C). The microgel core/shell structures are clearly visible; the silicon

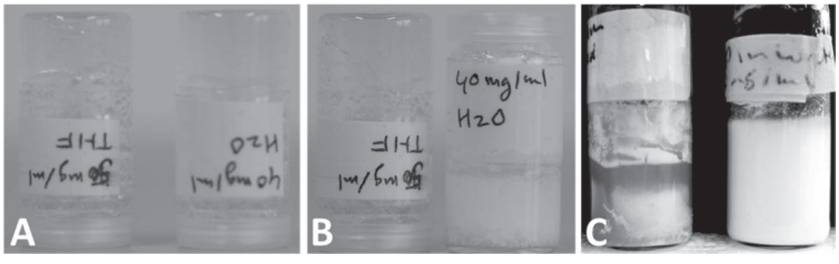

Figure 5. Photographs of the non-cross-linked gels in THF (left) and water (right) at ambient temperature (A) and 50° C (B). The THF gel remains stable and unaltered while the aqueous gel is transformed into a milky suspension. C) The cross-linked aqueous gels display a different behavior: Upon heating, the aqueous gel shrinks into a rubbery substance (left) while the non-cross-linked gel turns milky (right). Cross-linked gel in THF does not display any changes at higher temperature (not shown).

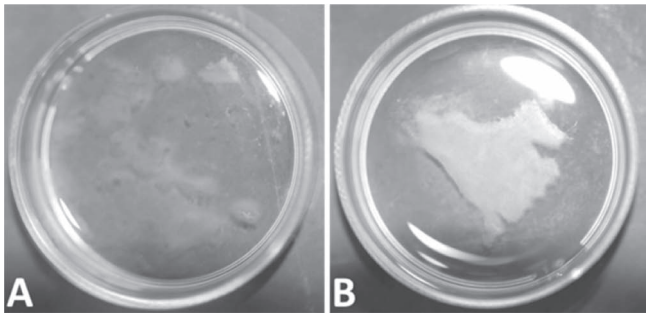

Figure 6. Thin hydrated SiO_2-PNIPAAm-DMIAAm films non-cross-linked (A) and cross-linked (B) floating on the water/air interface.

oxide nanoparticle in the middle is surrounded by the polymer corona. The diameters of the spherical structures (≈500 nm) are smaller than the non-cross-liked ones, which is in accordance with findings from cryo-SEM, indicating that the structures become smaller upon cross-linking. The packing is less dense as observed in cryo-SEM but the film is analyzed in the dry state and a closer packing can therefore be expected. After removing parts of the film by scratching with a cannula, the film thickness of the dried film can be analyzed. From the height profile, it can be seen that the thickness is in the range of about 155 nm (Figure 7B,C). Obviously, the microgel particles strongly deform upon drying on a solid substrate.

When the cross-linked thin film prepared from the temperature responsive core/shell structures is floated on top of the air/water interface, as shown in **Figure 8**A, it slowly turns from semitransparent to white and starts shrinking gradually upon raising the temperature to 50 °C (Figure 8B). It was found that upon cooling, the original state was recovered. Since the collapse and re-swelling of the SiO_2-PNIPAAm-DMIAAm film is associated with the expelling and re-uptake of water by the polymer shells, the aqueous phase was exchanged with a gold nanoparticle solution when the film was in its collapsed state (Figure 8B). Upon lowering the temperature, the film swells again, taking up the surrounding aqueous phase containing the gold nanoparticles, which can be seen as darker areas in Figure 8C. Though, the film is not homogeneously colored, it is clear that this is a straightforward and convenient way of incorporating additional functionalities into these macroscopic structures. The particles remain inside the film even after exchanging the nanoparticle solution for MilliQ-water and no apparent loss of color is visible, even after several days.

In order to prove that the gold nanoparticles are indeed incorporated into the microgel and not just adsorbed onto the surface, we performed TEM investigations. While these large and relatively thick films are difficult to analyze by TEM, a similar heat-cool cycle experiment in the presence of gold nanoparticles was performed with the individual microgels in solution. After the incorporation step, the microgels were isolated by selective precipitation via centrifugation. At low centrifugation speed, the microgels could be separated from left-over gold nanoparticles. The isolated microgels were slightly purple colored. Analysis by TEM showed indeed that the small gold nanoparticles are incorporated into the shell of the microgel (**Figure 9**).

While gold nanoparticles and nanorods are able to transform photonic energy into heat, a similar approach would be possible for silver nanoparticles (antibacterial/catalysis), platinum nanoparticles (catalysis), semiconductor nanoparticles (fluorescence), and even small molecular components such as antibiotics and other medicinal components, though in case of small molecules, diffusion out of the material after exchanging the solution will become more likely.

2.4. Responsive Self-Assembled Fibers

In addition to the approach of freeze-drying in combination with cross-linking it is also possible to prepare fiber-like materials. Here we used the cononsolvency properties of PNIPAAm.[52,53] While PNIPAAm becomes less soluble at elevated temperatures, it also becomes less soluble when certain cosolvents are added. In general these can be different alcohols[54,55] but also THF.[56,57] The solvent composition affects the LCST and in some compositions the transition temperature drops drastically, rendering PNIPAAm also insoluble at room and lower temperatures.[52] We used this property to extrude a THF gel of SiO_2-PNIPAAm-DMIAAm particles through a small diameter needle into a thin layer of hot water. The gel that is pushed out instantly forms a thin collapsed fiber and does not lose its integrity.[67] After the water is removed the particles inside the fibers are cross-linked with UV-light for about four hours. Upon rehydration by submersing them in water (**Figure 10**A), they

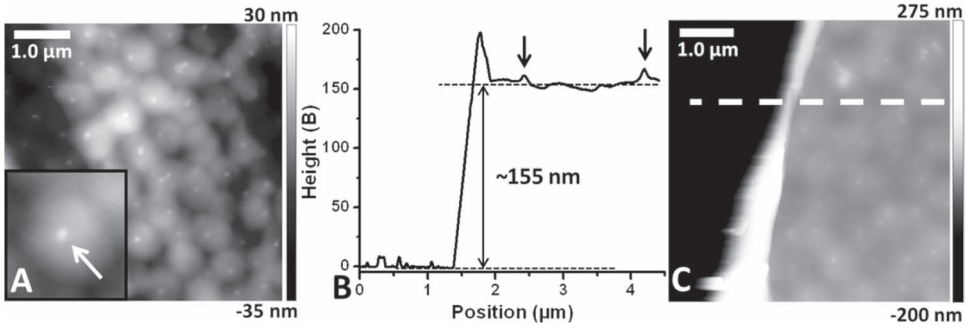

Figure 7. Dried cross-linked microgel film analyzed by SFM, which shows the height (A) and cross-section (B) of a scratched surface (C) and contours of closely packed core/shell structures displaying the silicon-core (indicating with arrows) surrounded by a polymer corona.

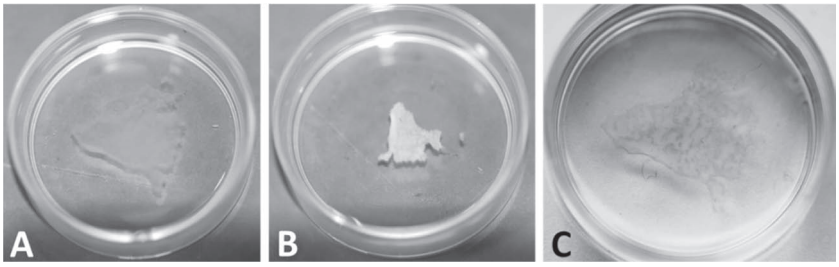

Figure 8. Photographs of a cross-linked film of SiO_2-PNIPAAm-DMIAAm at ambient temperature (A) and in the shrunken state at 50 °C (B). When the aqueous phase is exchanged for a gold nanoparticle solution in the collapsed state and cooled to room temperature the gold nanoparticles are readily taken-up by the film and remain there even after exchanging the solution for fresh pure water (C).

retain their integrity and are even strong enough to be taken out by tweezers (Figure 10B). The fibers are very hydrophilic, as can be inferred from the meniscus forming at the water/fiber interface. As soon as the fiber is completely removed from the water, it wraps around the tweezers until it is placed back into the water, where is retakes its shape.

The fibers, much like the particles and thin films, are also thermoresponsive, as increasing the temperature renders the fiber thinner and shorter (Supporting Information SI 4). Also, collapsing in an aqueous gold nanoparticle solution and slowly decreasing the temperature re-swells the fiber, taking up the nanoparticles. In **Figure 11**A, fibers with (dark) and without (slightly white) incorporated gold nanoparticles are shown in clean water. Analyzing the dried fiber by SEM reveals a diameter of about 900 µm (Figure 11B). Instead of being covered with gold nanoparticles homogenously, they appear in patches (Figure 11C,D). This straightforward approach of incorporation of different species would allow for the fabrication of multiresponsive and functional self-assembled cross-linked fibers.

This shows that collapsing-reswelling of the microgel via a heat-cool cycle is very efficient in incorporating additional particle functionalities. Thin films and fiber for materials such as membranes or responsive porous surfaces can easily be modified via this approach. We are currently investigating the viability of the approach to test for further incorporation of functional particles such as reactive nanoparticles or protein structures.

3. Conclusion

Core/shell microgel-like structures with responsive properties towards, e.g., temperature and pH, are promising for nanomaterials with possible applications in controlled drug-release systems,[58,59] biomedical applications,[60] biosensors,[61] responsive interfacial stabilization in e.g., Pickering emulsions,[62,63] and for the formation of stable capsules.[64] The properties found in this investigation extend these possible applications and functions to macroscopic materials. It was

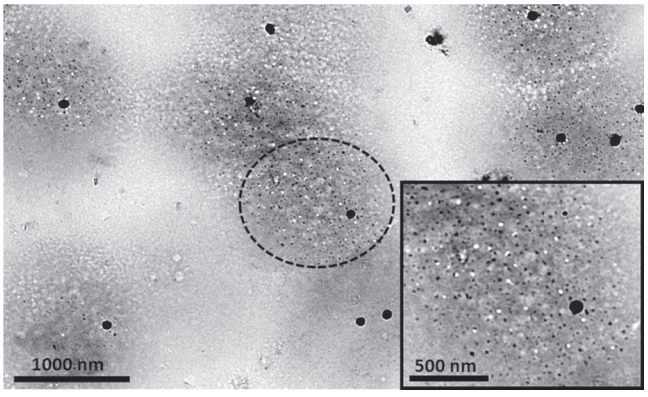

Figure 9. TEM analysis of gold nanoparticles incorporated into the core/shell microgels. The nanoparticles are confined to the shell of the microgel indicating that indeed the particles are taken-up via the heat-cool cycle. Dotted line indicates the gel-confined particles.

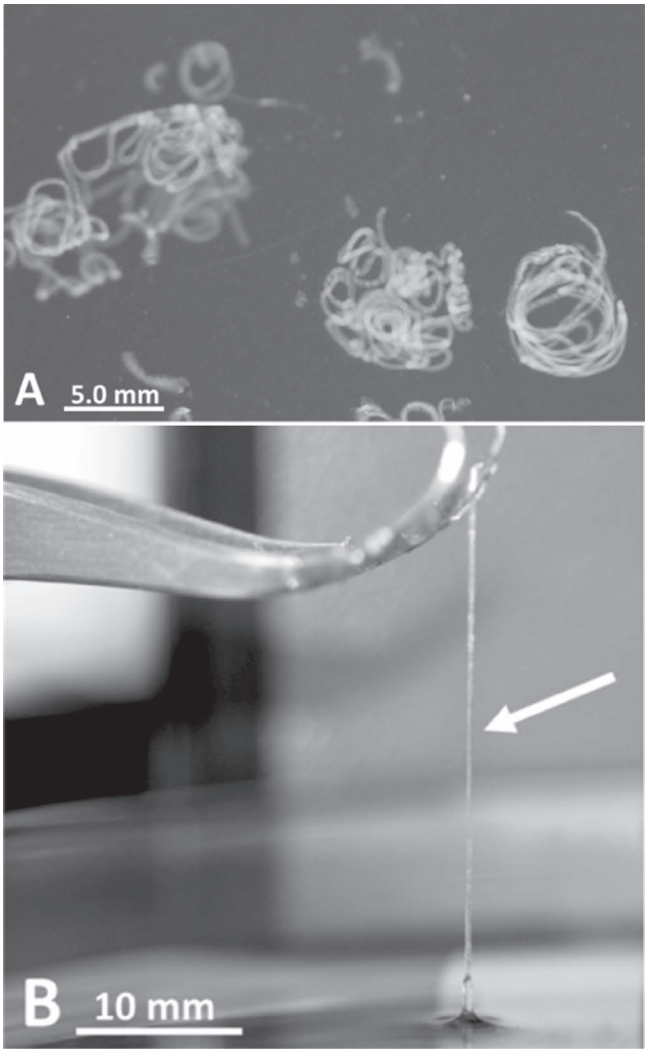

Figure 10. Photographs of fibers formed via extrusion of a THF gel of SiO_2-PNIPAAm-DMIAAm through a thin needle into hot water and are subsequently collected, irradiated with UV (cross-linked) and rehydrated (A). The fibers are strong enough to be pulled out of the water being very hydrophilic and highly flexible (B).

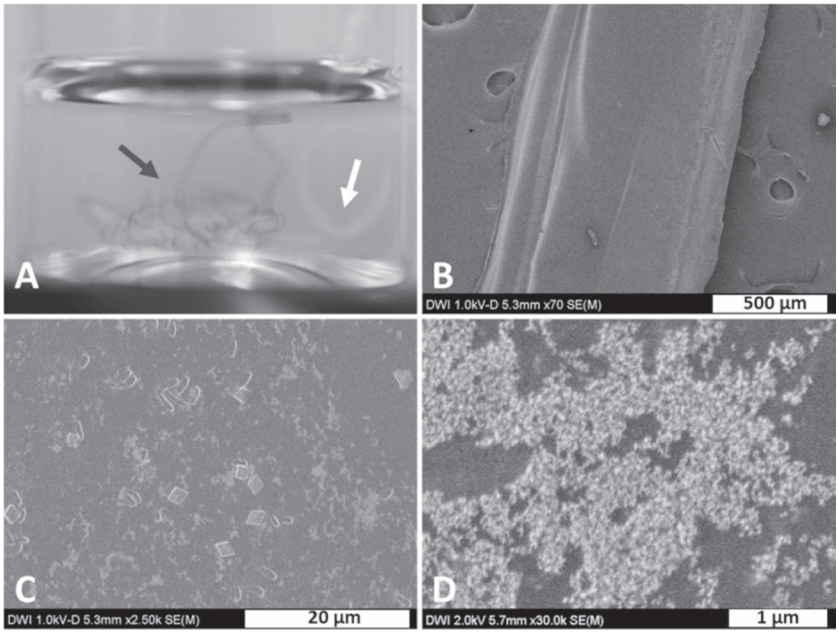

Figure 11. Photograph of two fibers, collapsed and re-swollen, in a gold nanoparticle solution and transferred to a clean aqueous phase (black arrow) together with a particle-free fiber (white arrow) (A). The difference in color, given by the incorporated gold nanoparticles is clearly noticeable. SEM images with different enlargements of a dried fiber that contains gold nanoparticles (B–D). The particles are not distributed evenly but appear in small patches across the fiber. The crystals observed in (C) are most likely salt.

found that for SiO_2-PNIPAAm-DMIAAm core/shell structures, of which the polymer corona is in the range of several hundreds of nanometers in thickness, the overall micrometer-sized structure is able to gelate various polar and non-polar solvents. In particular, water-based gels are of interest as aqueous systems as they have the possibility to be compatible with biological systems, are useful for medical applications, and THF in combination with water induces a co-nonsolvency effect. This effect was used here to produce easily processable fiber structures. The extruded fibers remain stable upon dilution due to the insolubility of the THF gel in water. The stability is of sufficient time to isolate the fibers and to cross-link the particles. The fibers are very flexible and other nanocomposites can be embedded into the fibers via an easy shrinking–swelling procedure. Thin films, which were prepared by freeze-drying in combination with UV cross-linking in the solid state, present equal opportunities. Both thin films and fibers have many potential applications and further investigations with respect to their application in embedding materials for cell adhesion, membranes, and responsive fibers are currently under investigation.

4. Experimental Section

General Information: Solvents (HPLC-grade) and chemicals were purchased from Sigma Aldrich and used without further purification unless stated otherwise. NIPAAm (99%, Aldrich) was purified by two successive recrystallizations in a mixture of n-hexane and benzene (4:1 v:v). The photoresponsive cross-linker was synthesized according to a literature procedure from Kuckling et al.[45] The gold nanoparticles where synthesized according to literature.[65] UV irradiation of the cross-linker was carried out with a 400 W UV lamp (Panacol 400F), with emitting light with a wavelength λ between 315 and 400 nm. TEM imaging was done by placing a drop of solution on a carbon-coated copper grid and subsequent removal of excess liquid with filtration paper after approximately 1 min in ambient atmosphere. The analysis was performed on a ZEISS LIBRA120 PLUS electron microscope, operating at 120 kV. (Cryo-)SEM images were taken using a Hitachi S-4800 field emission scanning electron microscope (FESEM) operating at 1–2 kV and 10 µA current. Samples for cryo-SEM were placed on a carbon-coated grid and plunged in liquid nitrogen for freezing. The images were obtained after partly sublimation of the surface. SFM images were taken on a Veeco Instruments scanning force microscope operating on Nanoscope software.

Synthesis SiO_2-Nanoparticles: The preparation of silica nanoparticles (SiNP) was carried out by the Stöber Method.[49] The average size obtained was about 60 nm. A mixture of pure ethanol (50 mL) and aqueous ammonia (29%) (4 mL) was heated to 60 °C and stirred at 100 rpm in a round flask equipped with a reflux condenser. After 30 min of equilibration time, tetraethoxysilane (TEOS) (1.5 mL) was added to the solution. The solution became turbid about 1 h after the addition of the TEOS. The resulting dispersion was stirred overnight at 60 °C. After 24 h the colloidal dispersion was cooled to room temperature, purified by centrifugation (30 min at 9000 rpm), and re-dispersed in pure ethanol (50 mL) (3 times in total).

Surface Modification of SiO_2-Nanoparticles with MPS: In order to functionalize the particles, the SiO_2-NP dispersion in ethanol (15 mL) was mixed with methacryloxypropyltrimethoxysilane (MPS) (15 µL) and stirred overnight at room temperature, followed by heating to 80 °C for 1 h to ensure covalent bonding. The functionalized particles were cooled to room temperature, purified by centrifugation (30 min at 9000 rpm), and re-dispersed in solvent (15 mL) (2× in ethanol followed by 2× in MilliQ- water).

Surface Polymerization: Synthesis of the polymer shell was carried out by conventional emulsion polymerization.[28] A degassed solution of NIPAAm (11.3 g, 100 mmol) and DMIAAm (1.0 g, 5 mmol) in MilliQ-water (800 mL) was prepared in a three-neck round flask equipped with a reflux condenser and the solution was heated to 40 °C. The SiO_2-NP dispersion was added to the emulsion which was then heated to 70 °C. After 1 h of equilibration time, aqueous potassium peroxodisulfate (KPS) solution (1 mL) (1 mg mL^{-1}) was added to start the polymerization. The emulsion became turbid after approximately 30 min. The polymerization was allowed to react for 4 h. The mixture was cooled to room temperature and stirred overnight. The SiO_2-PNIPAAm-DMIAAm particles were purified by centrifugation (60 min at 11 000 rpm) and re-dispersion in MilliQ-water.

Supporting Information

Supporting Information is available from the Wiley Online Library or from the author.

Acknowledgements

This project was financially supported by the Alexander von Humboldt-Foundation (PvR) and the Lichtenberg program of the VolkswagenStiftung (AB). Dr. Kim-Hô Phan is kindly acknowledged for the help concerning the cryo-SEM.

Received: November 21, 2011
Published online: February 10, 2012

[1] G. R. Hendrickson, M. H. Smith, A. B. South, L. A. Lyon, *Adv. Funct. Mater.* **2010**, *20*, 1697.
[2] A. Fernández-Barbero, I. J. Suárez, B. Sierra-Martín, A. Fernández-Nieves, F. J. de las Nieves, M. Marquez, J. Rubio-Retama, E. López-Cabarcos, *Adv. Colloid Interface Sci.* **2009**, *147–148*, 88.
[3] S. Nayak, L. A. Lyon, *Angew. Chem. Int. Ed.* **2005**, *44*, 7686.
[4] M. A. Cohen Stuart, W. T. S. Huck, J. Genzer, M. Müller, C. Ober, M. Stamm, G. B. Sukhorukov, I. Szleifer, V. V. Tsukruk, M. Urban, F. Winnik, S. Zauscher, I. Luzinov, S. Minko, *Nat. Mater.* **2010**, *9*, 101.
[5] G. Pasparakisa, M. Vamvakaki, *Polym. Chem.* **2011**, *2*, 1234.
[6] D. Kuckling, *Colloid Polym Sci.* **2009**, *287*, 881.
[7] M. E. Harmon, D. Kuckling, P. Pareek, C. W. Frank, *Langmuir* **2003**, *19*, 10947.
[8] O. D. Velev, S. Gupta, *Adv. Mater.* **2009**, *21*, 1897.
[9] D. Kuckling, J. Hoffmann, M. Plötner, D. Ferse, K. Kretschmer, H.-J. P. Adler, K.-F. Arndt, R. Reichelt, *Polymer* **2003**, *44*, 4455.
[10] S. Hiltl, M.-P. Schürings, A. Balaceanu, V. Mayorga, C. Liedel, A. Pich, A. Böker, *Soft Matter* **2011**, *7*, 8231.
[11] J.-H. Kim, T. R. Lee, *Chem. Mater.* **2004**, *16*, 3647.
[12] D. Kuckling, C. D. Vo, H.-J. P. Adler, A. Volkel, H. Colfen, *Macromolecules* **2006**, *39*, 1585.
[13] X. Dai, F. Zhou, N. Khan, W. T. S. Huck, C. F. Kaminski, *Langmuir* **2008**, *24*, 13182.
[14] K. Peng, I. Tomatsu, A. Kros, *Chem. Commun.* **2010**, *46*, 4094.
[15] a) P. van Rijn, D. Janeliunas, A. M. Brizard, M. C. A. Stuart, Ger J. M. Koper, a Rienk Eelkema, J. H. van Esch, *New J. Chem.* **2011**, *35*, 558; b) C. B. Minkenberg, F. Li, P. van Rijn, L. Florusse, J. Boekhoven, M. C. A. Stuart, G. J. M. Koper, R. Eelkema, J. H. van Esch, *Angew. Chem. Int. Ed.* **2011**, *50*, 3421; c) J. J. D. de Jong, P. van Rijn, T. D. Tiemersma-Wegeman, L. N. Lucas, W. R. Browne, R. M. Kellogg, K. Uchida, J. H. van Esch, B. L. Feringa, *Tetrahedron* **2008**, *64*, 8324.
[16] Y. Osada, J.-P. Gong, *Adv. Mater.* **1998**, *10*, 827.
[17] I. Dimitrov, B. Trzebicka, A. H. E. Müller, A. Dworak, C. B. Tsvetanov, *Prog. Polym. Sci.* **2007**, *32*, 1275.
[18] S. Fujishige, K. Kubota, I. Ando, *J. Phys. Chem.* **1989**, *93*, 3311.
[19] H. G. Schild, *Prog. Polym. Sci.* **1992**, *17*, 163.
[20] Z.-C. Wang, X.-D. Xu, C.-S. Chen, L. Yun, J.-C. Song, X.-Z. Zhang, R.-X. Zhuo, *ACS Appl. Mater. Interfaces* **2010**, *2*, 1009.
[21] W. Liu, B. Zhang, W. W. Lu, X. Lia, D. Zhu, K. De Yao, Q. Wang, C. Zhao, C. Wang, *Biomaterials* **2004**, *25*, 3005.
[22] R. Pelton, *Adv. Colloid Interface Sci.* **2000**, *85*, 1.
[23] M. Das, H. Zhang, E. Kumacheva, *Annu. Rev. Mater. Res.* **2006**, *36*, 117.
[24] J. K. Oh, R. Drumright, D. J. Siegwart, K. Matyjaszewski, *Prog. Polym. Sci.* **2008**, *33*, 4, 448.
[25] O. J. Cayre, N. Chagneux, S. Biggs, *Soft Matter* **2011**, *7*, 2211.
[26] H. Zhang, J. Han, B. Yang, *Adv. Funct. Mater.* **2010**, *20*, 1533.
[27] X. Hu, Z. Tong, L. A. Lyon, *J. Am. Chem. Soc.* **2010**, *132*, 11470.
[28] a) M. Karg, I. Pastoriza-Santos, L. M. Liz-Marzán, T. Hellweg, *Chem PhysChem* **2006**, *7*, 2298; b) M. Karg, T. Hellweg, *J. Mater. Chem.* **2009**, *19*, 8714.
[29] R. Contreras-Cáceres, J. Pacifico, I. Pastoriza-Santos, J. Pérez-Juste, A. Fernández-Barbero, L. M. Liz-Marzán, *Adv. Funct. Mater.* **2009**, *19*, 3070.
[30] X.-Q. Zhao, T.-X. Wang, W. Liu, C.-D. Wang, D. Wang, T. Shang, L.-H. Shen, L. Ren, *J. Mater. Chem.* **2011**, *21*, 7240.
[31] X. Yang, Y. Lu, *Mater. Lett.* **2005**, *59*, 2484.
[32] A. F. E. Hezinger, J. Teßmar, A. Göpferich, *Eur. J. Pharm. Biopharm.* **2008**, *68*, 138.
[33] N. A. D. Burke, H. D. H. Stöver, F. P. Dawson, *Chem. Mater.* **2002**, *14*, 4752.
[34] R. A. Frimpong, J. Z. Hilt, *Nanotechnology* **2008**, *19*, 175101.
[35] N. C. Mougin, P. van Rijn, H. Park, A. H. E. Müller, A. Böker, *Adv. Funct. Mater.* **2011**, *21*, 2470.
[36] Y. Hu, D. Chen, S. Park, T. Emrick, T. P. Russell, *Adv. Mater.* **2010**, *22*, 2583.
[37] J. Rodríguez-Fernández, M. Fedoruk, C. Hrelescu, A. A. Lutich, J. Feldmann, *Nanotechnology* **2011**, *22*, 245708.
[38] A. Travan, C. Pelillo, I. Donati, E. Marsich, M. Benincasa, T. Scarpa, S. Semeraro, G. Turco, R. Gennaro, S. Paoletti, *Biomacromolecules* **2009**, *10*, 1429.
[39] P. Dallas, V. K. Sharma, R. Zboril, *Adv. Colloid Interface Sci.* **2011**, *166*, 119.
[40] N. R. Jana, *Phys. Chem. Chem. Phys.* **2011**, *13*, 385.
[41] L. Sheeney-Haj-Ichia, G. Sharabi, I. Willner, *Adv. Funct. Mater.* **2002**, *12*, 27.
[42] M. Takafuji, S.-Y. Yamada, H. Ihara, *Chem. Commun.* **2011**, *47*, 1024.
[43] C. R. van den Brom, I. Anac, R. F. Roskamp, M. Retsch, U. Jonas, B. Mengesad, J. A. Preece, *J. Mater. Chem.* **2010**, *20*, 4827.
[44] C. Wang, N. T. Flynn, R. Langer, *Adv. Mater.* **2004**, *16*, 1074.
[45] L. Ling, W. D. Habicher, D. Kuckling, H.-J. Adler, *Des. Monomers Polym.* **1999**, *2*, 351.
[46] E. M. Benetti, X. F. Sui, S. Zapotoczny, G. Julius Vancso, *Adv. Funct. Mater.* **2010**, *20*, 939.
[47] a) S. Schmidt, M. Zeiser, T. Hellweg, C. Duschl, A. Fery, H. Möhwald, *Adv. Funct. Mater.* **2010**, *20*, 3235; b) M. E. Nash, W. M. Carroll, N. Nikoloskya, R. Yang, C. O' Connell, A. V. Gorelov, P. Dockery, C. Liptrot, F. M. Lyng, A. Garcia, Y. A. Rochev, *ACS Appl. Mater. Interfaces* **2011**, *3*, 1980.
[48] H. Zhang, X. Lei, Z. Su, P. Liu, *J. Polym. Res.* **2007**, *14*, 253.
[49] W. Stöber, A. Fink, E. Bohn, *J. Colloid Interface Sci.* **1968**, *26*, 62.
[50] P. Xu, H. Wang, R. Tong, Q. Du, W. Zhong, *Colloid Polym Sci.* **2006**, *284*, 755.
[51] a) K. A. Dawson, *Curr. Opin. Colloid Interface Sci.* **2002**, *7*, 218; b) F. Mammeri, E. Le Bourhis, L. Rozes, C. Sanchez, *J. Mater. Chem.* **2005**, *15*, 3787.
[52] H. G. Schild, M. Muthukumar, D. A. Tirrell, *Macromolecules* **1991**, *24*, 948.
[53] F. Tanaka, T. Koga, *Phys. Rev. Lett.* **2008**, *101*, 028302.
[54] C. Scherzinger, P. Lindner, M. Keerl, W. Richtering, *Macromolecules* **2010**, *43*, 6829.
[55] F. Tanaka, T. Koga, H. Kojima, N. Xue, F. M. Winnik, *Macromolecules* **2011**, *44*, 2978.
[56] J. Hao, H. Cheng, P. Butler, L. Zhang, C. C. Han, *J. Chem. Phys.* **2010**, *132*, 154902.
[57] F. M. Winnik, M. F. Ottaviani, Stefan H. Boßmann, W. Pan, M. Garcia-Garibay, N. J. Turro, *Macromolecules* **1993**, *26*, 4577.
[58] H. Otsuka, Y. Nagasaki, K. Kataoka, *Adv. Drug Delivery Rev.* **2003**, *55*, 403.
[59] M. Malmsten, H. Bysell, P. Hansson, *Curr. Opin. Colloid Interface Sci.*. **2010**, *15*, 435.
[60] Y. Guan, Y. Zhang, *Soft Matter* **2011**, *7*, 6375.
[61] L. J. Nielsen, L. F. Olsen, V. C. Ozalp, *ACS Nano* **2010**, *4*, 4361.
[62] L. Isa, E. Amstad, K. Schwenke, E. Del Gado, P. Ilg, M. Kröger, E. Reimhult, *Soft Matter* **2011**, *7*, 7663.
[63] B. Brugger, S. Rütten, K.-H. Phan, M. Möller, W. Richtering, *Angew. Chem. Int. Ed.* **2009**, *48*, 3978.
[64] P. van Rijn, N. C. Mougin, D. Franke, H. Park, A. Böker, *Chem. Commun.* **2011**, *47*, 8376.
[65] B. V. Enustun, J. Turkevich, *J. Am. Chem. Soc.* **1963**, *85*, 3317.
[66] a) G. V. Schulz, G. Harborth, *Makromol. Chem.* **1948**, *1*, 106; b) E. Trommsdorff, H. Kohel, P. Lagally, *Makromol. Chem.* **1948**, *1*, 169; c) P. R. Dvornić, M. S. Jaćović, *Polym. Eng. Sci.* **1981**, *21*, 792.
[67] Extruding in water at ambient temperature produces thicker fibers. However, it was found that increasing the temperature results in denser fiber. While in this process, the solvent composition inside the fiber cannot be controlled precisely, it yields better results than just injecting an aqueous gel into hot water.